Extension of the angular spectrum method to model the pressure field of a cylindrically curved array transducer

Natalia Ilyina[1,2], Jeroen Hermans[3], Koen Van Den Abeele[4], Jan D'hooge[1]

[1]Dept. of Cardiovascular Sciences, KU Leuven, Leuven, Belgium; [2]Institute for Environment, Health and Safety, Belgian Nuclear Research Centre SCK•CEN, Mol, Belgium; [3]DoseVue NV, Hasselt, Belgium; [4]Dept. of Physics, KU Leuven Kulak, Kortrijk, Belgium.

Abstract: An extension to the angular spectrum approach for modelling pressure fields of a cylindrically-curved array transducer is described in this paper. The proposed technique is based on representing the curved transducer surface as a set of planar elements whose contributions are combined at a selected intermediate plane from which the field is further propagated using the conventional angular spectrum approach. The accuracy of the proposed technique is validated through comparison with Field II simulations.

1. Introduction

The angular spectrum approach (ASA) has been widely used to model pressure fields generated by ultrasonic transducers [1-5]. This method makes use of a two-dimensional Fourier transform to propagate the pressure field in-between parallel planes and is known to be highly computationally efficient and easy in implementation. For wave propagation in a homogeneous media, the ASA has been shown to be equivalent to other simulation methods such as directly solving the Rayleigh-Sommerfeld integral or ones based on the spatial impulse response method [6-8]. While the Rayleigh-Sommerfeld integral method is relatively time-consuming, the spatial impulse response method intrinsically assumes linear wave propagation in an acoustically homogeneous medium. In contrast, the ASA can be extended to include nonlinear effects and to model pressure fields in layered (i.e. inhomogeneous) media [2-3].

In order for the ASA to be applied, knowledge of the field distribution on the source plane is required. Although this problem is straightforward for planar transducer geometries, it is not for curved transducers as used in many medical applications to improve focusing. In this paper, we propose an extension of the angular spectrum method to a case of a cylindrically curved array transducer as commonly used in medical ultrasound imaging. This technique provides easy means for analysis and interpretation of acoustic fields radiated from such transducers and is inspired by the method that was recently proposed for a spherically curved transducer [4].

The procedure described in Ref. [4] consists of dividing the transducer surface into a set of planar concentric rings, each contained within a plane parallel to a selected intermediate plane in front of the transducer. The angular spectrum of each ring is calculated separately and propagated to this intermediate plane, where the contributions of all rings are added. Subsequently, the intermediate plane is used as the source plane for sound field estimation using the conventional ASA.

The purpose of this paper was therefore to demonstrate the application of a similar strategy as the one proposed by Vyas & Christensen in order to compute the spectrum of a cylindrically curved array transducer. First, the calculation procedure is described, followed by the comparison of the numerical results to those obtained with Field II [7].

2. Method

Herein, a cylindrically curved ultrasonic array was considered with N_{el} elements (N_{el} is assumed to be even) of height H and width W, with a zero kerf and a radius of curvature R. The intermediate plane was defined as tangential to the transducer's aperture and perpendicular to the $x-z$ plane (Fig. 1 (a)). Next, all transducer elements were subdivided along the elevation direction into $(2N_y+1)$ small sub-elements that can be regarded as planar rectangles of height $\Delta y = \frac{H}{2N_y+1}$. It should be noted that given dense sampling and moderate curvature of the transducer aperture, the sub-elements can be considered parallel to the $x-z$ plane. This assumption greatly simplifies the calculations, since the angular spectrum of each sub-element can be calculated in the same coordinate space.

The angular spectrum of such sub-element centered at (x_m, y_n), where $m=-N_{el}/2,...,N_{el}/2$ and $n=-N_y,...,N_y$, is given by:

$$V_{m,n}(k_x,k_y)=\int_{x_m-\frac{W}{2}}^{x_m+\frac{W}{2}}\int_{y_n-\frac{\Delta y}{2}}^{y_n+\frac{\Delta y}{2}} e^{-j(k_x x+k_y y)}dxdy, \quad (1)$$

where k_x and k_y are the spatial frequencies.

Substituting $\tilde{x}=\frac{x-x_m}{W}$ and $\tilde{y}=\frac{y-y_n}{\Delta y}$ we obtain:

$$V_{m,n}(k_x,k_y)=\int_{-\frac{1}{2}}^{\frac{1}{2}}\int_{-\frac{1}{2}}^{\frac{1}{2}} W\Delta y e^{-j(k_x W\tilde{x}+k_y \Delta y\tilde{y})}e^{-j(k_x x_m+k_y y_n)}d\tilde{x}d\tilde{y}=e^{-j(k_x x_m+k_y y_n)}\frac{4\sin\left(k_x\frac{W}{2}\right)\sin\left(k_y\frac{\Delta y}{2}\right)}{k_x k_y}. \quad (2)$$

As seen in Fig. 1 (b), the travel distance z_n from each sub-element to the intermediate plane depends on the sub-element's elevational coordinate. Propagation of each sub-element's angular spectrum to the intermediate plane is modelled using the following transfer function [1]:

$$H_{el,n}=\left(e^{-jk_z z_n}\right)^*, \quad (3)$$

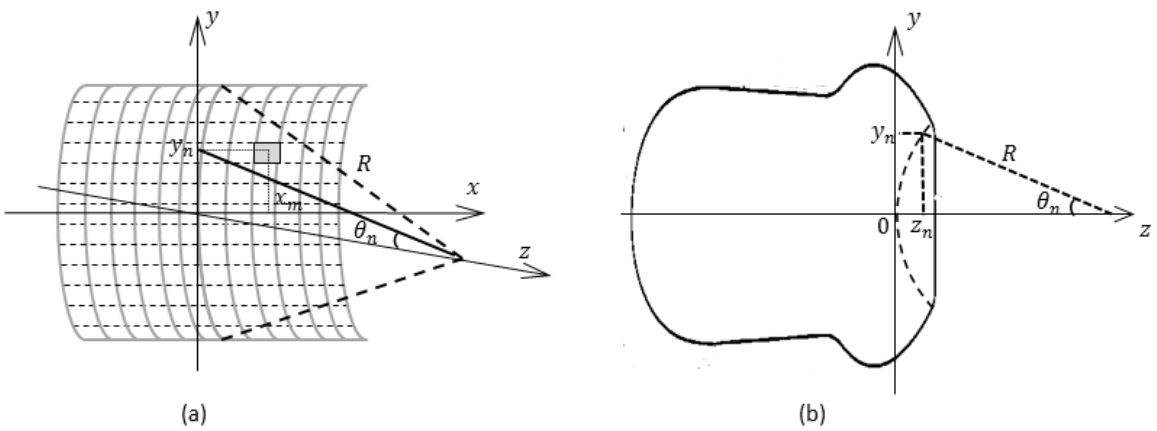

Figure 1. Representation of a cylindrically-curved linear array transducer by a set of planar rectangles: 3-D view (a) and cross-sectional view (b).

where $k_z = \sqrt{k^2 - \left(k_x^2 + k_y^2\right)}$ and $k = \omega/c$ is the wave number for the angular frequency ω and speed of sound c and '*' indicates the complex conjugate. As can be seen from Fig. 1(b), the travel distance is given by: $z_n = R(1-\cos\theta_n)$. The above transfer function accounts for a phase difference due to the difference in horizontal propagation distance for an element with the elevational coordinate y_n with respect to the central element.

Azimuthal focusing is accounted for by introducing a phase factor determined by the azimuthal coordinate of the sub-element:

$$H_{az,m} = e^{-j\omega t_m}, \tag{4}$$

where t_m is the transmit time delay of the m[th] transducer element, which for a one-dimensional array is given by:

$$t_m = \frac{d_F - \sqrt{\left(x_m - x_F\right)^2 + {z_F}^2}}{c}, \tag{5}$$

with d_F the distance from the center of the aperture to the focal point and x_F and z_F – the azimuthal and axial coordinates of the focal point.

Finally, the angular spectrum of the entire transducer aperture on the intermediate plane can be calculated by adding the contributions of all sub-elements (N_{el} in the azimuthal and $2N_y+1$ in the elevational directions):

$$V(k_x, k_y : \omega) = \sum_{n=1}^{(2N_y+1)} \sum_{m=1}^{N_{el}} V_{n,m} H_{el,n} H_{az,m}. \tag{6}$$

Substituting Eq. (2), (3) and (4) into Eq. (6), we get:

$$V(k_x,k_y:\omega)=\frac{4\sin\left(k_x\frac{W}{2}\right)\sin\left(k_y\frac{\triangle y}{2}\right)}{k_xk_y}\sum_{n=-N_y}^{N_y}\left[e^{-jk_yy_n}\left(e^{-jk_zz_n}\right)^*\right]\sum_{m=1}^{N_{el}}\left[e^{-jk_xx_m}e^{-j\omega t_m}\right], \quad (7)$$

The first summation on the right-hand side can be rewritten as follows:

$$\sum_{n=-N_y}^{N_y}\left[e^{-jk_yy_n}\left(e^{-jk_zz_n}\right)^*\right]=1+\sum_{n=1}^{N_y}\left[2\cos(k_yn\Delta y)\left(e^{-jk_zz_n}\right)^*\right]. \quad (8)$$

The pressure field distribution in any plane that is parallel to the intermediate plane at distance z can be determined by multiplying the source angular spectrum in Eq. (7) with the following transfer function [1]:

$$H\left(k_x,k_y,z:\omega\right)=\left(\frac{je^{jzk_z}}{k_z}\right)^*, \quad (9)$$

and taking the 2-D inverse Fourier transform of the resulting spatial-frequency distribution.

3. Numerical simulation

In order to validate the above expressions, a phased array transducer with a cylindrically curved aperture was modelled using both the above approach and with Field II (based on the spatial impulse response method) [7]. The transducer aperture consisted of 64 $\left(N_{el}\right)$ elements of 12 mm × 0.22 mm (corresponding to H and W), and a kerf of zero between the transducer elements was assumed. The radius of the elevation curvature (R) was set to 70 mm and the electronic focus was set at $\left[x_{F,}y_F,z_F\right]=\left[0,0,70mm\right]$. For the ASA modelling, the number of aperture sub-elements along the elevation direction $\left(2N_y+1\right)$ was set to 55 ($\Delta y=\Delta x=\lambda/2=0.22$ mm, where $\lambda=0.44$ mm is the wavelength). In Field II, the function "xdc_focused_array" was used to model the transducer, and the transducer aperture was subdivided into 55 sub-elements in elevational and 1 in azimuthal direction (corresponding to the same sub-element size as used for the ASA: 0.22 mm × 0.22 mm).

The pressure field propagation was modelled in a homogeneous medium with a speed of sound of 1540 m/s. A Gaussian-modulated sinusoidal pulse of 1.5 periods, 3.5 MHz center frequency and 80% relative bandwidth was generated in Field II and was used as the input for the angular spectrum simulations. For both simulators, a sampling frequency of 100 MHz was used. For the ASA simulations, a 1024-point fast Fourier transform was applied to a time-domain pulse; the pressure field was simulated for non-zero frequency components of the spectrum (70 in this case). Propagation of the pressure field using the ASA was modelled in the spatial-frequency domain and an angular restriction was applied to avoid aliasing effects [5].

4. Results

Figure 2 compares the azimuthal and elevational transmit beam profiles at the focal depth and the axial RMS pressure profiles obtained with both simulators showing very good agreement

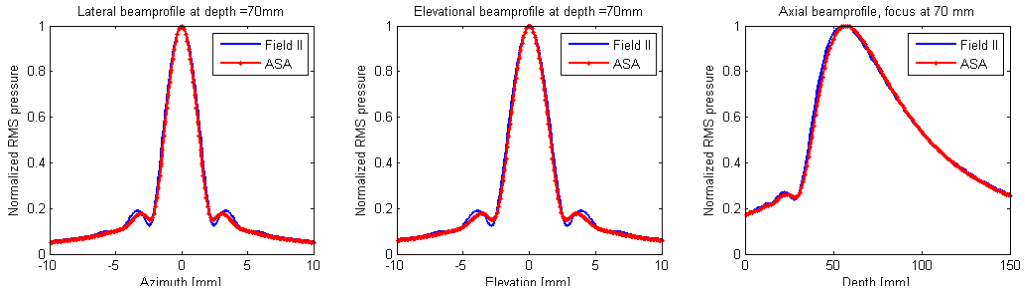

Figure 2. Comparison of the simulated transmit beam profiles of a focused linear array transducer obtained with ASA and Field II: lateral (a), elevational (b) and axial (c). Transducer element size: 0.22 mm x 12 mm, number of elements – 64, center frequency – 3.5 MHz, elevational focus – 70 mm, azimuthal focus – 70 mm, measurement depth of transverse plots – 70 mm.

between both simulation approaches. The comparison of the (normalized) transmit RMS pressure fields is presented in Fig. 3. Overall, the simulated pressure fields look very similar with a maximal percentage difference of normalized patterns below 6 %.

All simulations were performed on a computer with an Intel Core i7 2.7 GHz processor and 8 GB physical memory. The estimates of the computation time for both simulation methods are summarized in the Table.

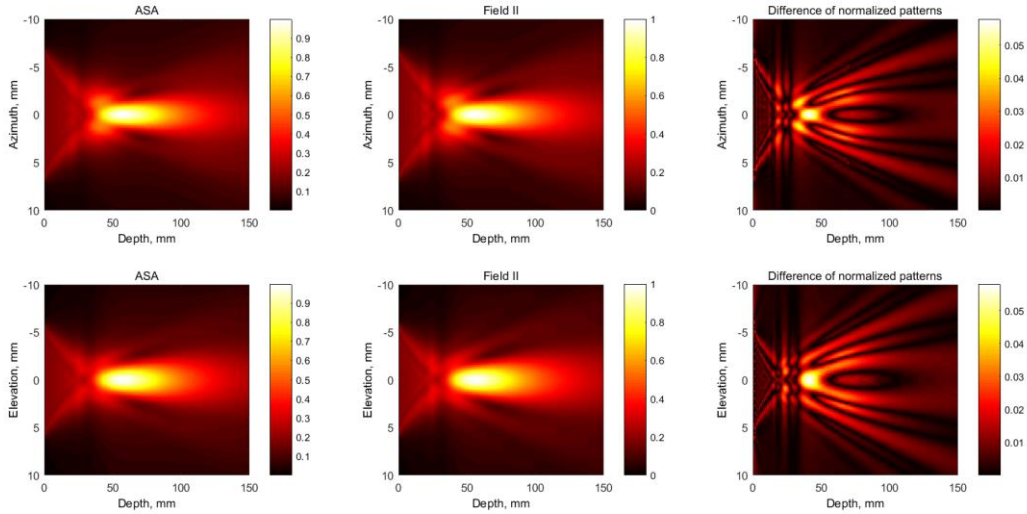

Figure 3. Comparison of the simulated transmit pressure fields of a focused linear array transducer obtained with ASA and Field II: in the azimuthal plane (upper row) and elevational plane (lower row). Transducer element size: 0.22 mm x 12 mm, number of elements – 64, center frequency – 3.5 MHz, elevational focus – 70 mm, azimuthal focus – 70 mm, measurement range – 1-150 mm.

5. Conclusion

The recently proposed method for modelling spherically curved transducer apertures with ASA was reformulated for the case of cylindrically curved arrays. The method divides the transducer aperture into a set of planar rectangular sub-elements, the angular spectrum of which is

calculated separately and propagated to a preselected intermediate plane in which the contributions of all sub-elements are combined. The accuracy of the derived expressions was validated through comparison with Field II simulations. As expected, Field II showed faster performance during the computation of pulsed acoustic excitation, while the ASA was more efficient during field computations in a plane parallel to the transducer surface. It should be noted, that these time estimates are purely indicative since the implementation of the proposed ASA approach was done in a MATLAB environment (The MathWorks Inc., Natick, MA, USA) while Field II executes its core calculations in C. Obviously, the proposed method can thus be further optimized using compiled computer languages and effective parallel programming using a multi-core computer or a graphical processing unit. Overall, this study demonstrates that the proposed technique provides an easy means for modelling pressure fields of commonly used transducers for clinical practice that can be extended to consider inhomogeneous media and embedded nonlinear effects.

Table. Computation time required for the simulations in Field II and ASA.

	Field II (broadband)	ASA	
		(broadband, i.e. 70 frequency points)	Centre frequency only
Lateral beam profiles	0.95 s	11.7 s	0.22 s
Axial beam profile	0.09 s	1948 s	25.6 s
Field distribution in a plane parallel to the transducer (70 mm)	545 s	59 s	2.0 s

References

[1] J. W. Goodman, *Introduction to Fourier optics* (McGraw-Hill, New York, 1968).

[2] P. T. Christopher and K. J. Parker, "New approaches to the linear propagation of acoustic fields", J. Acoust. Soc. Am., **90**, 507-521 (1991).

[3] R. J. Zemp, J. Tavakkoli and R.S.C. Cobbold, "Modeling of nonlinear ultrasound propagation in tissue from array transducers", J. Acoust. Soc. Am., **113**, 139-51 (2003).

[4] U. Vyas and D. A. Christensen, "Extension of the angular spectrum method to calculate pressures from a spherically curved acoustic source", J. Acoust. Soc. Am., **130**, 2687-2693 (2011).

[5] P. Wu, R. Kazys, and T. Stepinski, "Optimal selection of parameters for angular spectrum approach to numerically evaluate acoustic fields", J. Acoust. Soc. Am., **101**, 125-134 (1997).

[6] E. S. Ebbini and C. A. Cain, "Multiple-focus ultrasound phased-array pattern synthesis: optimal driving-signal distributions for hyperthermia", IEEE Trans. Ultrason. Ferroel. Freq. Contr., **36,** 540-548 (1989).

[7] J. A. Jensen and N. B. Svendsen, "Calculation of pressure fields from arbitrarily shaped, apodized, and excited ultrasound transducers*",* IEEE Trans. Ultrason. Ferroel. Freq. Contr., **39,** 262-267 (1992).

[8] P. Stepanishen, M. Forbes, and S. Letcher, "The relationship between the impulse response and angular spectrum methods to evaluate acoustic transient fields", J. Acoust. Soc. Am., **90**, 2794-2797 (1991).